**Ocean Systems Engineering**, *Vol. 15, No. 1 (2025) 23-42*
https://doi.org/10.12989/ose.2025.15.1.023 

# Development of variable-fidelity FOWT digital twins in extreme sea environments: Part I – mid-fidelity analysis

Hyoungchul Kim*[1], Ikjae Lee[2], Moohyun Kim[2], Hyunchul Jang[1] and Bonjun Koo[1]

*[1]TechnipEnergies, 15377 Memorial Dr, Houston, TX 77079, USA*
*[2]Department of Ocean Engineering, Texas A&M University, Haynes Engineering Building, 727 Ross St, College Station, TX 77843, USA*

*(Received December 17, 2024, Revised February 15, 2025, Accepted March 2, 2025)*

**Abstract.** In the coming years, more Floating Offshore Wind Turbines (FOWT) are projected to be installed beyond the continental shelf in the USA and worldwide. Accurate and reliable modeling of various environmental loadings and the resulting dynamic responses are crucial for the structural design, operation, and safety of FOWTs. To develop accurate and reliable FOWT design tools, a collaborative effort between academia (Texas A & M University), industry (Technip Energies), and class society (American Bureau of Shipping), supported by the Ocean Energy Safety Institute (OESI), has been undertaken. In this project, accurate and reliable digital twin (DT) models were developed based on the high-fidelity CFD models and mid-fidelity potential-flow models. In the mid-fidelity models, the wind turbine and platform dynamically interact, exchanging loads and motions at each time step. Aerodynamic loadings on the blade elements, considering wind-inflow data, tower and blade elasticity, and blade-pitch control are included. Hydrodynamic loading is calculated using potential-flow theory with Morison's equation, and the FEM is used to model the behavior of mooring lines. The present study is presented in two separate papers. This paper, Part I, focuses on the development and validation of two mid-fidelity DT models (OrcaFlex and MLTSIM-OpenFAST) for a 15MW semi-submersible wind turbine model. The results from the two mid-fidelity DT simulations were verified through several system identification tests and for various extreme environmental conditions. In future work, the capabilities of these models will be extended to consider the effects of submarine earthquakes and tsunami waves, expanding the design loading cases of current design guidelines.

**Keywords:** digital twins; FOWT; mid-fidelity fully coupled numerical analysis; validation

## 1. Introduction

Floating Offshore Wind Turbines (FOWTs) represent a pivotal advancement in harnessing renewable energy from offshore wind resources. As these structures evolve to meet growing energy demands, the design and maintenance complexities associated with their dynamic environments necessitate advanced analytical methodologies. Traditional frequency domain approaches, commonly employed for global performance and structural analysis of floating offshore platforms, face challenges in accurately capturing the intricate non-linear interactions

*Corresponding author, Ph.D., E-mail: hyoungchul.kim@ten.com


http://www.techno-press.org/?journal=ose&subpage=7 ISSN: 2093-6702 (Print), 2093-677X (Online)

between the RNA (rotor nacelle assembly), tower, and substructure with mooring inherent in FOWTs.

In response to these challenges, this study presents a cutting-edge approach: fully-coupled time domain analysis, which enhances the precision and efficiency of FOWT design and maintenance using digital twins. Unlike frequency domain methods, time domain analysis offers a more accurate representation of the coupled dynamic behavior of FOWTs, considering the strong non-linear coupling with control that defines their mechanical responses. To develop accurate and reliable FOWT design tools, a collaborative effort between academia (Texas A & M University), industry (Technip Energies), and class society (American Bureau of Shipping), supported by the Ocean Energy Safety Institute (OESI), has been undertaken. The FOWT selected for this study has semi-submersible-type floating foundation with 15MW turbine very similar to IEA 15MW generic turbine (Gaertner *et al*. 2020) designed by Technip for 1000 m water depth.

A digital twin (DT) is a precise virtual representation of a physical object. It leverages real-time analytics to create virtual models that assess the condition of real systems and identify causal relationships. These virtual models can also forecast outcomes by applying various input parameters expected to occur in real systems soon. Recently, digital twins have been explored as a novel method for predicting wind turbine outputs. Studies on digital twin technology for wind turbines have enhanced operational conditions by developing techniques for fault diagnosis, condition monitoring, and residual life prediction for floating wind turbines. Once a physics-based model is established for the digital twin, it becomes straightforward to analyze and validate various input data and compute complex systems like wind turbines in near real-time.

For instance, several papers examine the global performance of various types of floating offshore wind turbines in real environments using mid-fidelity tools based on potential theory. These studies use a coupled dynamic analysis program to simulate the system and compare the results with model tests. The findings show a reasonable correlation between the numerical simulations and the experimental data, validating the numerical model's effectiveness (Robertson *et al.* 2023, Kim *et al.* 2016, 2017). Additionally, Liu *et al.* (2023) develops a DT framework for the floating wind turbines by integrating physical and digital processes during the installation and O&M phases. Branlard *et al.* (2024) presents a physics-based digital twin validated with data from the TetraSpar prototype, exploring the integration of mid-fidelity and high-fidelity models to improve predictive maintenance strategies.

In this project, accurate and reliable DT models were developed based on the high-fidelity CFD (computational fluid dynamics) models and mid-fidelity potential-flow-based models. The mid-fidelity DT is useful, after fine tuning against high-fidelity DT, in repeated calculations with varying design parameters to find the optimal design, repeated runs of the optimized design for various wind-wave-current conditions to generate synthetic data to train relevant ML (machine learning) algorithms, and simultaneous run for comparison with physical twin during operation. In the mid-fidelity models, the wind turbine and floating platform dynamically interact, exchanging loads and motions at each time step. Aerodynamic loadings on the blade elements, considering wind-inflow data, tower and blade elasticity, and blade-pitch control are included. Hydrodynamic loading is calculated using potential-flow theory with Morison's equation to empirically account for viscous drag forces, and the FEM (finite element method) is used to model the behavior of mooring lines. In this paper, two mid-fidelity DT models are employed and used for cross-checking. One is based on a commercial FOWT analysis software, OrcaFlex, developed by Orcina. The other is based on MLTSIM-OpenFAST, developed by Technip Energies (T.EN). The OpenFAST was developed by NREL (National renewable Energy Lab) (Jonkman *et al*. 2011) and

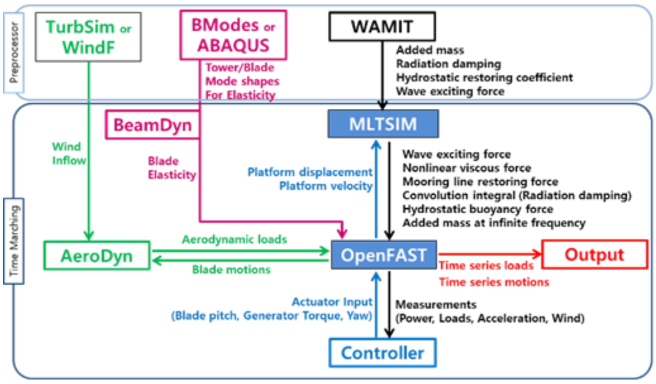


Fig. 1 MLTSIM-OpenFAST Flowchart

its turbine part was exploited through external coupling in MLTSIM-OpenFAST.

The present study is presented in two separate papers. This paper, Part I, focuses on the development and validation of two mid-fidelity DT models (OrcaFlex and MLTSIM-OpenFAST) for a 15 MW semi-submersible wind turbine model. The results from the two mid-fidelity DT simulations were verified through several system identification tests (e.g. static-offset and free-decay numerical tests) and for various ocean environmental conditions. Another paper, Part II, focuses on the development and validation of the CFD-based high-fidelity DT model, and the CFD simulation results were used to calibrate the empirical coefficients of the mid-fidelity tools presented in the present paper.

## 2. Numerical model for mid-fidelity digital twin

### *2.1 MLTSIM-OpenFAST model*

MLTSIM-OpenFAST utilizes OpenFAST for aero-servo-elasto-dynamics and MLTSIM for hydrodynamic loads and mooring system dynamics. Hydrodynamic coefficients are calculated using WAMIT, a commercial potential flow simulation software, and transferred to MLTSIM for time-domain analysis. The mooring loads are calculated using the Roddyn subroutine in MLTSIM, which is capable of simulating the visco-elastic behavior of synthetic mooring lines, as well as performing nonlinear finite element analysis for mooring lines, rigid risers, and flexible risers including power cables. OpenFAST calculates the wind turbine dynamics, including aerodynamic loads, elastic responses of the turbine tower, and the 6-DOF rigid body floating platform structural inertia and gravity loads. To calculate hydrodynamic and mooring loads on the floating platform, OpenFAST calculates the 6-DOF floater motions and velocities at every time step and passes them to MLTSIM, which calculates and returns the hydrodynamic loads and mooring loads to OpenFAST. The coupling between OpenFAST and MLTSIM is illustrated in Fig. 1.

MLTSIM-OpenFAST has been validated using the OC3 DeepCwind model test data from the Year 2012, and it can be utilized to analyze fully coupled dynamic responses of the wind turbine, floating platform, mooring lines, and power cables (Koo *et al*. 2012, 2013, 2014, Goupee *et al*. 2012). In addition, a floating wind turbine's life-cycle loading and operability analyses can be done

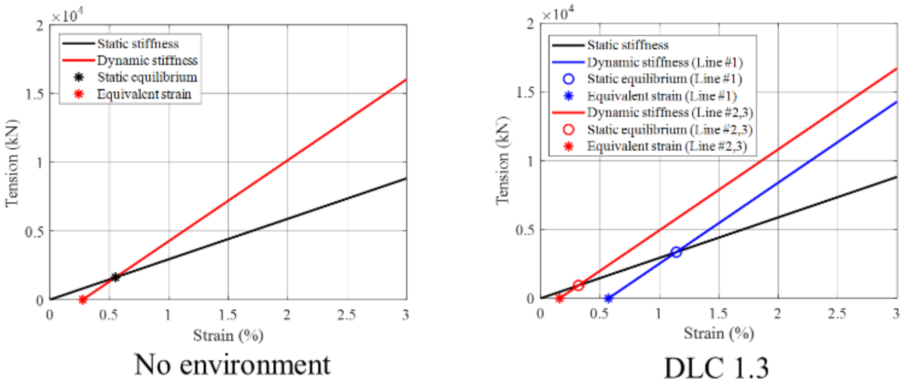


Fig. 2 Dual stiffness approach: Tension vs strain curves (static & dynamic stiffness)

with High Performance Computing (HPC) systems (Koo *et al*. 2015). MLTSIM-OpenFAST has a unique capability to use HPC efficiently which significantly reduces analysis time compared to other software for this type of simulations.

### *2.2 OrcaFlex model*

OrcaFlex, a commercially available software, performs global static and dynamic analysis of a wide range of FOWT systems, typically including boundary conditions such as vessels, buoys, etc., as well as finite element modeling of line structures. The long-established hydrodynamic capabilities of OrcaFlex can be coupled with a built-in aerodynamic turbine model, providing a fully coupled dynamic analysis tool suitable for both fixed and floating offshore wind turbines (Orcina. 2018). Additionally, it has capabilities comparable to OpenFAST. The rotor performance of the IEA 15 MW reference WTG model has been validated against OpenFAST results, showing very good agreement, as documented in Pell (2023). The WTG model is integrated with towers and substructures suitable for 15-MW-scale wind turbines. To implement hull hydrodynamics, frequency-domain analysis results, including 1st- and 2nd-order wave loads, are obtained from WAMIT and transferred to the OrcaFlex "vessel" object for time-domain analysis. Furthermore, in the program, a typical rigid floating platform-based FOWT analysis can easily be extended to account for the effect of hull flexibility on the FOWT's global performance based on multi-body hydrodynamics analysis (Lee *et al*. 2025).

### *2.3 Mooring models comparison – Dual stiffness vs Visco-elastic models*

The use of synthetic fiber, such as polyester, causes complexity in mooring dynamic analysis due to the time-dependent deformation behavior of synthetic fiber lines. Currently in the industry, the Dual-Stiffness (DS) model is used to consider this visco-elasticity effect of polyester ropes. In a Dual-Stiffness model, the total stretch of the polyester is given as a combination of quasi-static stretch driven by mean current, mean wind, and mean wave drift force which follows Hooke's law based on the static stiffness and dynamic stretch due to gust, wave and vortex-induced vibration (VIV) that follows Hooke's law based on dynamic stiffness. Global performance (or seakeeping)

Fig. 3 Schematic of 15 MW FOWT Model

simulation of a floating platform is performed in the time domain with mooring line stiffness given by the dynamic stiffness (or storm stiffness). The quasi-static stretch due to the mean load is considered by an increase in the length of the polyester rope equal to the difference between stretches due to static stiffness and dynamic stiffness of the polyester rope. Fig. 2 exhibits the loading condition-dependent stiffness values implemented in the DT models.

An alternative approach, i.e., the Visco-Elastic (VE) mooring model, is used for more accurate representation of the viscoelastic effects of polyester materials (Kim *et al*. 2010, Webster *et al*. 2012). The model accommodates basic properties of a polyester rope such as relaxation, creep, strain-stress hysteresis and frequency dependent stiffness. A Visco-Elastic model is defined using three parameters: static stiffness, dynamic stiffness, and τ. The static stiffness and dynamic stiffness have the same definitions as in the dual-stiffness model. The new parameter τ, which is called relaxation time, controls the transient time that the polyester rope requires to reach quasi-static stiffness. The Visco-Elastic model provides accurate platform offset prediction without any approximation on the mean environmental load and can simulate the transient effect due to the loss of a mooring line during storm conditions, which has not been possible to simulate using existing dual-stiffness models. In this study, OrcaFlex utilizes the Dual-Stiffness model, while MLTSIM-OpenFAST primarily employs the Visco-Elastic model, with dual-stiffness model also included in the irregular wave simulations.

## 3. Description of FOWT model

### *3.1 15 MW Floating Offshore Wind Turbine (FOWT)*

Fig. 3 shows a schematic of the floating wind turbine platform analyzed in this study with the wind turbine located atop one of the substructure columns. The wind turbine model is based on the IEA 15MW Wind Turbine (WT) model. The same Rotor Nacelle Assembly (RNA) is used, but the tower properties are modified for matching the modal properties to a T.EN in-house WT model. The WT is supported by T.EN's three-column semi-submersible floating platform designed by T.EN. The WT definitions are summarized in Table 2. For blade pitch and torque controls of the

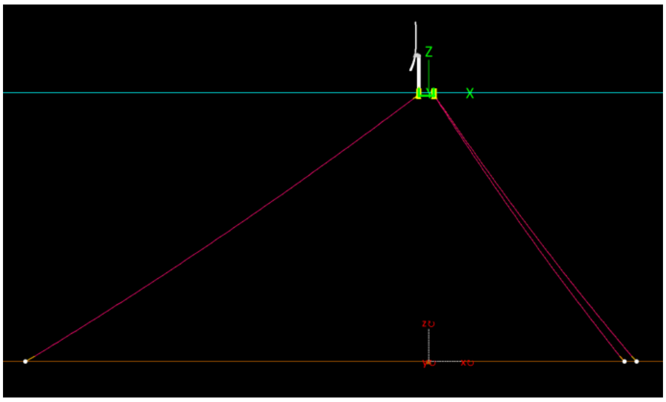

Fig. 4 Mooring Lines Layout: Side view

Table 2 15 MW Wind Turbine Specification

| Parameter | Unit | Value | Parameter | Unit | Value |
|---|---|---|---|---|---|
| Power rating | MW | 15 | Rotor diameter | m | 240 |
| Rotor orientation | - | Upwind | Design tip-speed ratio | - | 90 |
| Number of blades | - | 3 | Maximum rotor speed | rpm | 7.56 |
| Rated wind speed | m/s | 10.59 | Maximum tip speed | m/s | 95 |
| Cut-in wind speed | m/s | 3.0 | Blade mass | t | 65 |
| Cut-out wind speed | m/s | 25.0 | RNA mass | t | 1,017 |
| Hub height | m | 140 | Tower mass | t | 860 |
| Hub diameter | m | 7.94 | Tower base diameter | m | 10 |
| Hub overhang | m | 11.35 | Rated Power | MW | 15 |

wind turbine, the ROSCO controller developed by National Renewable Energy Lab (NREL) is used.

### 3.2 Mooring system

The FOWT DT model developed in this study is assumed to be installed in the deep sea of the Northern California area, with a water depth of 1000 meters. The mooring system is designed based on the ABS criteria (ABS, 2024). Three taut mooring lines are used for the 1000m water depth. Each mooring leg consists of an upper chain, a polyester rope, and a bottom chain without any buoyancy module, as shown in Fig. 4. The lengths of the upper chain, polyester, and lower chain are 20 m, 1700 m, and 40 m, respectively. The azimuth angles of the mooring lines as shown in Fig. 5 are defined with zero degrees along the positive x-axis and positive clockwise. The pretensions of mooring lines are 9.5% of the minimum breaking load (MBL). The properties and dimensions of the mooring lines are summarized in Table 3.

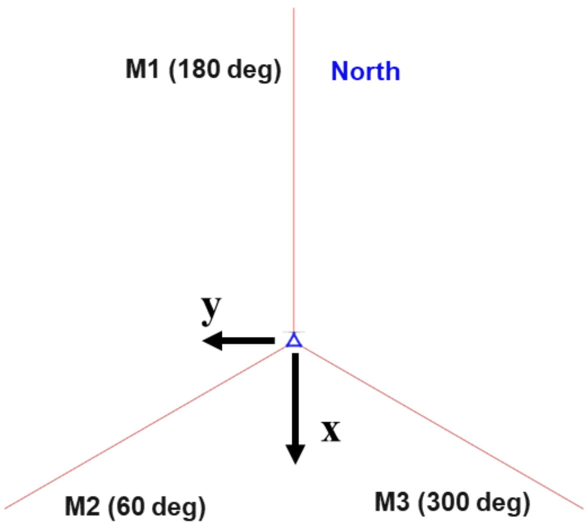


Fig. 5 Mooring Lines Layout: Birds-eye view

Table 3 Mooring Line Properties and Dimensions

| Parameter | | Unit | Value |
|---|---|---|---|
| **Water Depth** | | m | 1000 |
| **Diameter** | **Chain** | mm | 150 |
| | **Polyester Rope** | | 259 |
| **Length** | **Upper Chain** | m | 20 |
| | **Polyester Rope** | | 1700 |
| | **Bottom Chain** | | 40 |
| **MBL** | **Chain** | kN | 20956 |
| | **Polyester Rope** | | 19613 |
| **Pretension** | | kN | 2000 |
| **Horizontal Distance from Fairlead to Anchor** | | m | 1462 |
| **Mooring Azimuth Angle** | | deg | 60/180/300 |
| **Departure Angle at fairlead from MWL** | | deg | 38.33 |

### *3.3 Environmental Conditions*

Table 4 summarizes the selected Design Load Cases (DLCs) based on standard design guides. These load cases are based on met-ocean analysis data for the target site in Northern California, provided by ABS (ABS, 2012). For wind conditions, the analysis uses a 1-hour mean wind speed. The turbulent intensity (TI) for operational conditions and the wind speed for Extreme conditions are adjusted based on the guidelines from ABS (ABS, 2023).

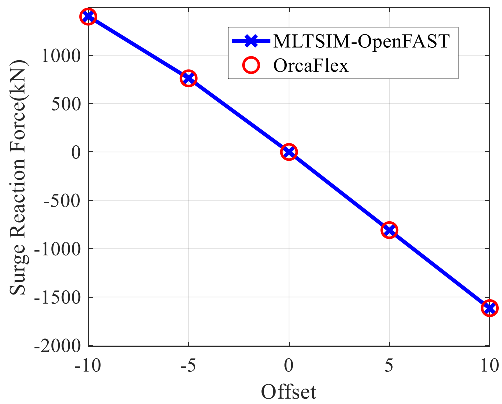


Fig. 6 Surge static offset test result comparisons

Table 4 Environmental conditions for operational and extreme conditions

| Title | | Unit | Operational | Extreme |
|---|---|---|---|---|
| **Wave** | **Hs** | **m** | 2.56 | 12.62 |
| | **Tp** | **sec** | 12 | 19.96 |
| | **gamma** | **(-)** | 1 | 1 |
| **Current** | **Depth - Speed** | **m - m/s** | 0 - 0.5<br>61 - 0.5<br>91 - 0.1<br>999 - 0.1 | 0 - 0.8<br>90 - 0.8<br>999 - 0.7 |
| **Wind** | **Vhub** | **m/s** | 10.59 | 34.58 |
| | **TI** | **%** | 30.73 | (-) |
| | **Power Law Coef.** | **(-)** | 0.14 | (-) |
| | **Spectrum** | | IEC-Kaimal | API-NPD |
| **DLC code** | | | 1.3 | 6.1 |

## 4. System identification

### *4.1 Static offset and free decay tests*

In order to ensure accuracy in the numerical modeling of the mooring lines, the static offset simulation results using static stiffness were compared between the OrcaFlex and MLTSIM-OpenFAST models. Fig. 6 presents static offset test results from MLTSIM-OpenFAST and OrcaFlex DT models. They agree very well. The natural periods and total damping are obtained from free decay simulations.

The drag coefficients for the platform structures such as the columns and pontoons are tuned based on the decay test results in high-fidelity CFD-based DT simulations, which can be found in the Part II of this study. The calibrated drag coefficients are summarized in Table 5. Fig. 7 show 6-DOFs free decay motion comparisons. The comparisons of the natural periods from MLTSIM-OpenFAST and OrcaFlex analysis are summarized in Table 6. Overall simulated natural

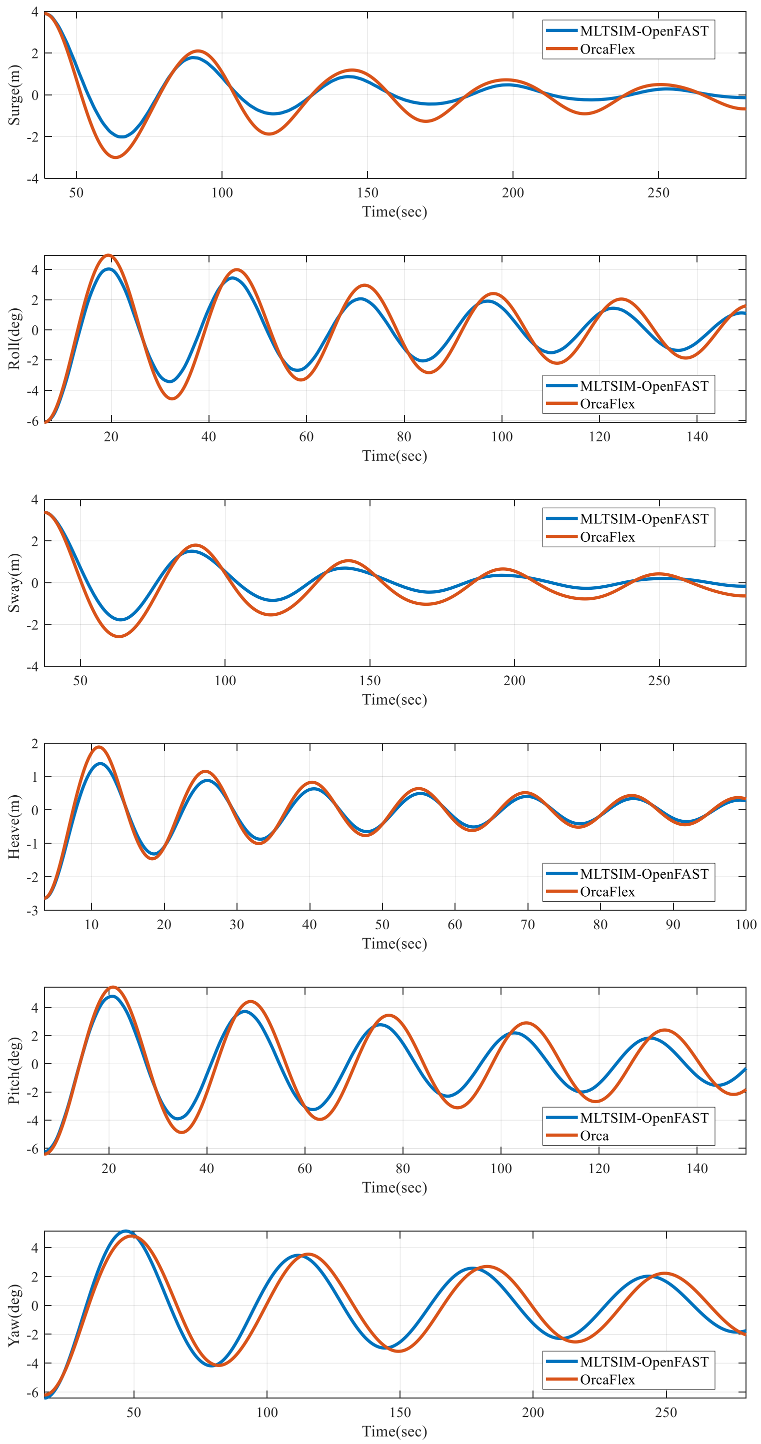


Fig. 7 Comparison of 6-DOFs Free Decay Test Results

Table 5 Drag Coefficients for Platform

| Parameter | | Drag Coefficient |
|---|---|---|
| **Column** | **Horizontal** | 1.00 |
| | **Vertical** | 1.10 |
| **Pontoon** | **Horizontal** | 1.58 |
| | **Vertical** | 5.00 |

Table 6 Natural Periods from Free Decay Tests (sec)

| 6-DOFs | MLTSIM-OpenFAST | OrcaFlex |
|---|---|---|
| **Surge** | 54.33 | 52.87 |
| **Sway** | 54.07 | 52.83 |
| **Heave** | 14.65 | 14.67 |
| **Roll** | 26.02 | 26.30 |
| **Pitch** | 27.53 | 28.13 |

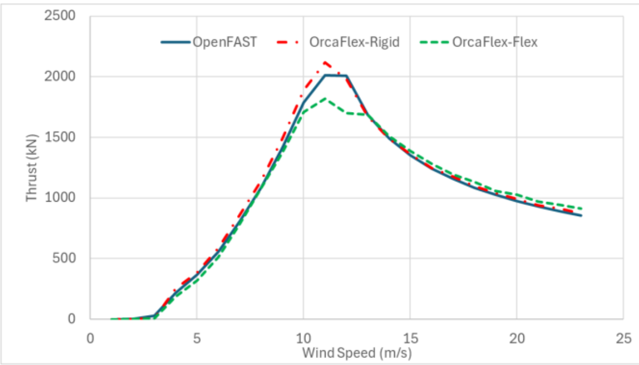


Fig. 8 Comparison of Thrust Forces on Fixed Wind Turbine

periods agree well between the two model analysis results. The OrcaFlex model results show slightly higher natural periods in the rotational DOF motions. Note that MLTSIM-OpenFAST uses the VE mooring model and OrcaFlex uses the DS mooring model for the decay tests comparison.

### *4.2 Wind turbine performance curve*

The wind thrusts based on a fixed wind turbine is compared between the MLTSIM-OpenFAST and OrcaFlex models. For this comparison, a step wind test was carried out on the fixed wind turbine, with the controllers for blade pitch and torque activated. Wind speed is increased in 1 m/s intervals from 0 m/s to 23 m/s, with each constant wind speed maintained for 200 seconds and each transient period lasting 100 seconds. In the ElastoDyn module of OpenFAST which calculates

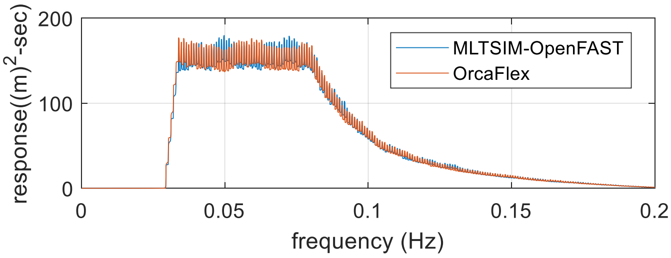


Fig. 9 Wave Elevation PSD for White Noise Simulation

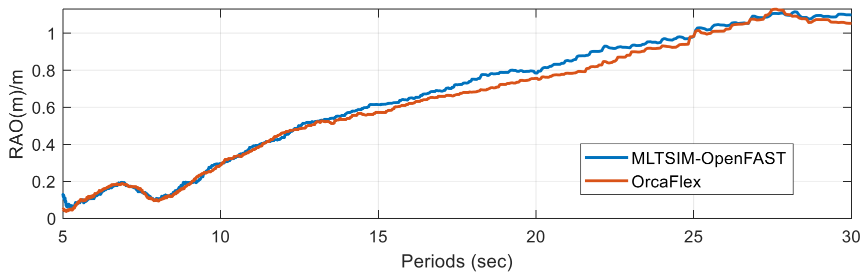


Fig. 10 Surge RAO

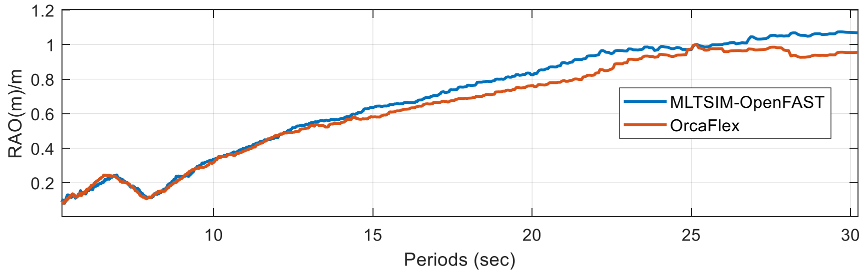


Fig. 11 Sway RAO

rotor dynamics with flexibility, the torsional mode is not included while OrcaFlex includes the torsional mode. This omission in ElastoDyn results in differences in the corresponding blade pitch angles at various wind speeds, leading to an overestimation of the thrust force near the rated wind speed, as illustrated in Fig. 8.

## 5. White-noise wave simulations

In this section, the FOWT motion RAO results are compared using the white-noise wave simulation. The linear and nonlinear wave response characteristics of the semi-submersible floating wind turbine were analyzed using white noise simulations. Fig. 9 shows the comparison between the white-noise wave spectra generated in MLTSIM-OpenFAST and OrcaFlex. In the white-noise simulations, a total of 200 white-noise wave components were used for the three-hour time domain simulations. Fig. 10 through Fig. 15 show RAO comparisons of the 6-DOFs motions.

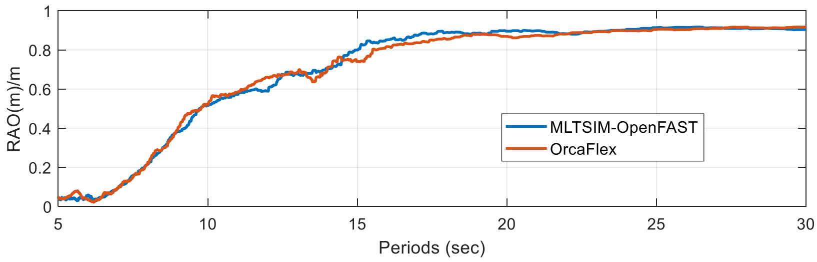


Fig. 12 Heave RAO

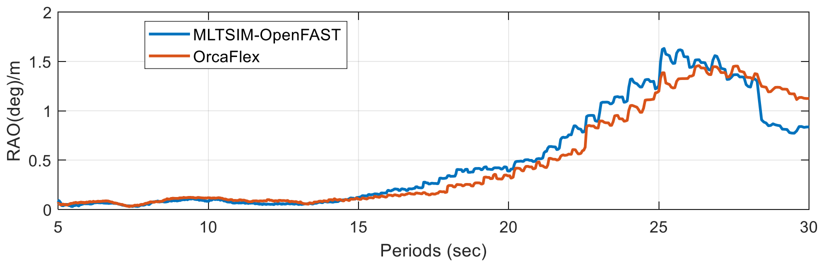


Fig. 13 Roll RAO

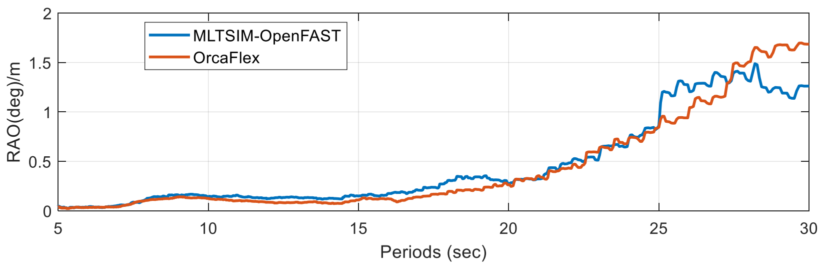


Fig. 14 Pitch RAO

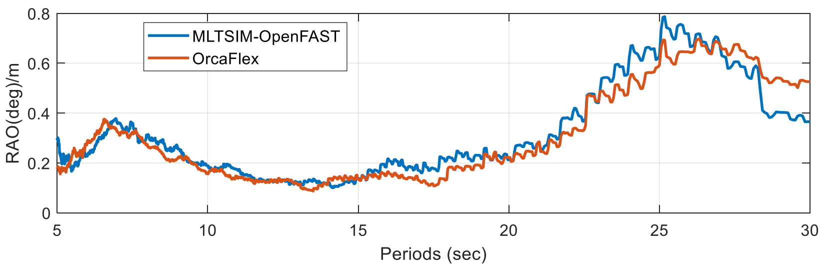


Fig. 15 Yaw RAO

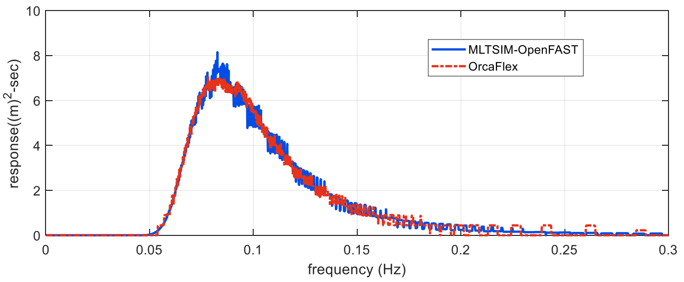


Fig. 16 Wave Elevation PSD in Operational Condition

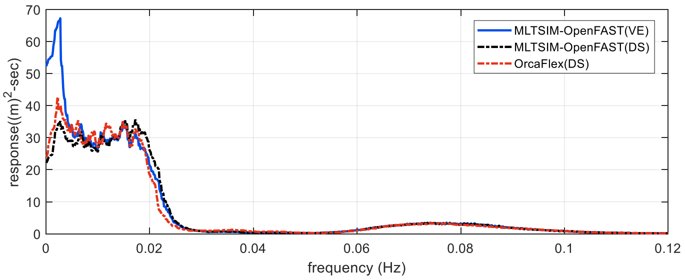


Fig. 17 Surge PSD in Operational Condition

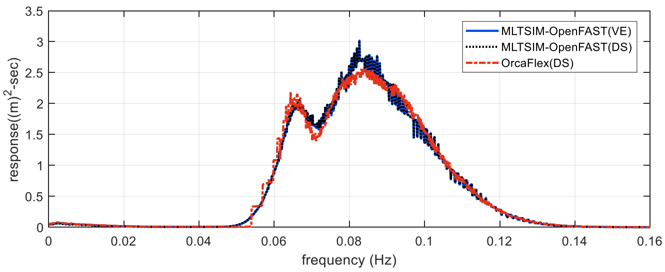


Fig. 18 Heave PSD in Operational Condition

The RAOs for 6-DOFs are slightly greater in MLTSIM-OpenFAST compared to OrcaFlex, but the differences are acceptable. The results generally show that the 6-DOF responses captured by MLTSIM-OpenFAST agree well with OrcaFlex results.

## 6. Irregular wave simulations

### *6.1 Operational condition*

Metocean conditions for the Design Load Cases (DLCs) of operating conditions based on ABS

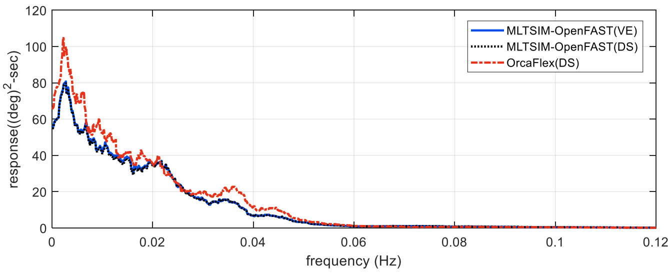


Fig. 19 Pitch PSD in Operational Condition

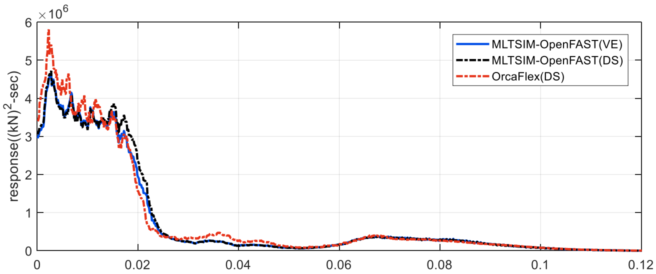


Fig. 20 Line #1 Mooring Tension PSD in Operational Condition

guidance (ABS, 2023) are presented in Table 4. The irregular waves are presented with JONSWAP spectra, and 200 wave components are used, and wave power spectral density (PSD) curves for OrcaFlex and MLTSMI-OpenFAST simulations matched well, as shown in Fig. 16. In the operational condition, the rated wind speed, 10.56 m/s, at hub height is selected because the maximum thrust occurs at the rated wind speed. The dynamic winds are generated using IEC-Kaimal wind spectrum with 30.73% TI.

Fig. 17 to Fig. 23 present the PSDs of surge, heave, and pitch motions, mooring tension, and fore-aft shear force, axial force, and bending moment at the tower base from MLTSIM-OpenFASTand OrcaFlex analyses. These PSDs are derived from a 3-hour irregular wave simulation. In the surge motion, the dual-stiffness models of OrcaFlex and MLTSIM-OpenFAST over-predict mean surge slightly, which means the estimated mean environmental force and mean stretch of the polyester rope is slightly higher than the actual values. MLTSIM-OpenFAST exhibits slightly higher low-frequency excitation with the Visco-Elastic polyester model. This discrepancy may stem from the dual-stiffness model's mean surge over-prediction or the Visco-Elastic model's transient effect on slow-varying surge motion under high low-frequency wind energy. Further study is needed to investigate this difference. The difference in low-frequency surge excitation is not significant enough to affect the mooring tension as shown in Fig. 20.

In the heave, mooring tension, and internal loading PSDs, results between MLTSIM-OpenFAST and OrcaFlex matched well. In the pitch PSD, OrcaFlex showed slightly higher excitation, but the difference was minimal. This indicates that the thrust differences at rated wind speed do not significantly affect global performance. Table 7 summarizes PSD statistics for 3-DOF motions (surge, heave, pitch), mooring tension, and internal loading (fore-aft shear force, axial force, fore-aft tower bending moment).

### *6.2 Extreme condition*

Metocean conditions for the Design Load Cases (DLCs) of extreme conditions based on ABS guidance (ABS, 2023) are presented in Table 4. The irregular waves are presented with JONSWAP spectra, and 200 wave components are used. Fig. 24 presents the JONSWAP wave spectra in MLTSIM-OpenFAST and OrcaFlex simulations, which matched well. The dynamic winds are generated using API-NPD wind spectrum with rated wind speed of 34.58 m/s at hub height.

Fig. 25 through Fig. 30 present the PSDs of surge, heave, and pitch motions, mooring tension, and fore-aft shear loading, axial loading and bending moment on the tower base from the MLTSIM-OpenFAST and OrcaFlex analyses. Under extreme conditions, PSD results for the 3-DOF motions, internal loading, and mooring tension matched well between MLTSIM-OpenFAST and OrcaFlex. In the pitch PSD, OrcaFlex slightly underestimates the peak pitch frequency and overestimates pitch excitation in slow-varying motion. The free-decay test shows a higher pitch natural period in OrcaFlex, which may cause the pitch PSD difference. Table 8 summarizes the statistics for 3-DOF motions (surge, heave, pitch), mooring tension, and internal loading (fore-aft shear force, axial force, fore-aft tower bending moment).

Table 7 Statistics of Motions, Mooring Tension, and Internal Loading on Tower Base in the Operational Condition

| Title | | Unit | Mean | Max | STD |
|---|---|---|---|---|---|
| Wave | MLTSIM-OpenFAST | (m) | 0.00 | 2.84 | 0.64 |
| | OrcaFlex (DS) | (m) | 0.00 | -2.50 | 0.64 |
| Surge | MLTSIM-OpenFAST (VE) | (m) | 9.70 | 13.23 | 1.00 |
| | MLTSIM-OpenFAST (DS) | (m) | 11.17 | 14.33 | 0.92 |
| | OrcaFlex (DS) | (m) | 11.01 | 14.32 | 0.91 |
| Heave | MLTSIM-OpenFAST (VE) | (m) | -0.09 | -1.32 | 0.32 |
| | MLTSIM-OpenFAST (DS) | (m) | -0.13 | -1.30 | 0.32 |
| | OrcaFlex (DS) | (m) | -0.23 | -1.44 | 0.32 |
| Pitch | MLTSIM-OpenFAST (VE) | (deg) | -5.74 | -9.81 | 1.24 |
| | MLTSIM-OpenFAST (DS) | (deg) | -5.71 | -9.56 | 1.23 |
| | OrcaFlex (DS) | (deg) | -5.90 | -9.89 | 1.34 |
| Line1 Tension | MLTSIM-OpenFAST (VE) | (kN) | 3.48E+03 | 4.55E+03 | 3.08E+02 |
| | MLTSIM-OpenFAST (DS) | (kN) | 3.60E+03 | 4.67E+03 | 3.13E+02 |
| | OrcaFlex (DS) | (kN) | 3.35E+03 | 4.50E+03 | 3.17E+02 |
| FA Shear Force | MLTSIM-OpenFAST (VE) | (kN) | 3.30E+03 | 6.37E+03 | 7.57E+02 |
| | OrcaFlex | (kN) | 3.35E+03 | 7.00E+03 | 8.31E+02 |
| Axial Shear Force | MLTSIM-OpenFAST (VE) | (kN) | -1.78E+04 | -1.63E+04 | 3.65E+02 |
| | OrcaFlex | (kN) | -1.86E+04 | -1.64E+04 | 4.53E+02 |
| FA Bending Moment | MLTSIM-OpenFAST (VE) | (kN-m) | 3.31E+05 | 6.75E+05 | 8.42E+04 |
| | OrcaFlex | (kN-m) | 2.90E+05 | 6.56E+05 | 9.13E+04 |

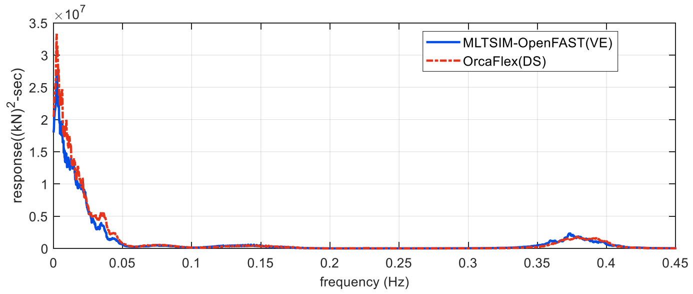


Fig. 21 Fore-Aft Shear Force PSD on Tower Base in Operational Condition

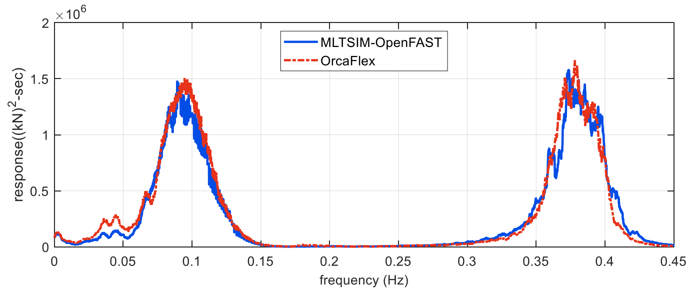


Fig. 22 Axial Shear Force PSD on Tower Base in Operational Condition

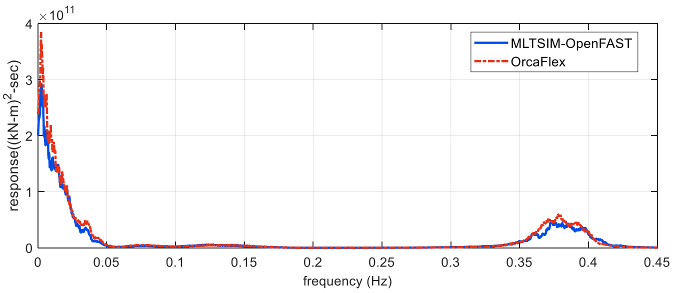


Fig. 23 Fore-Aft Bending Moment PSD on Tower Base in Operational Condition

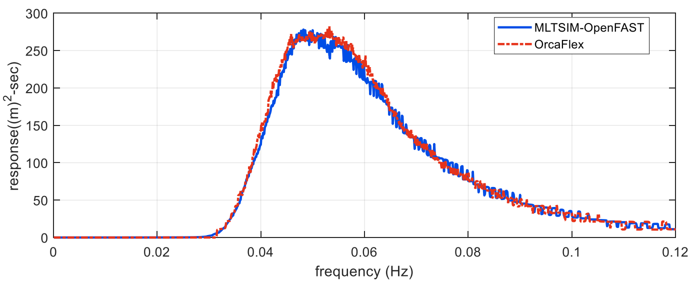


Fig. 24 Wave Elevation PSD in Extreme Condition

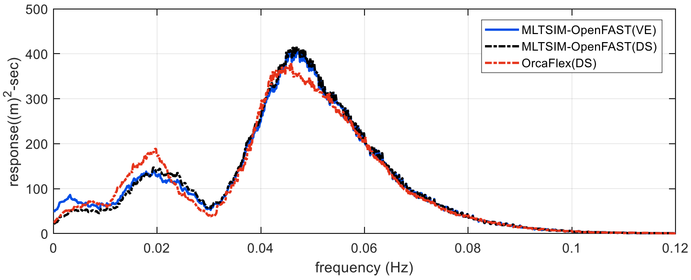


Fig. 25 Surge PSD in Extreme Condition

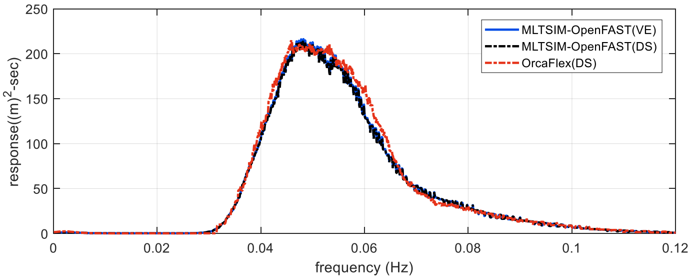


Fig. 26 Heave PSD in Extreme Condition

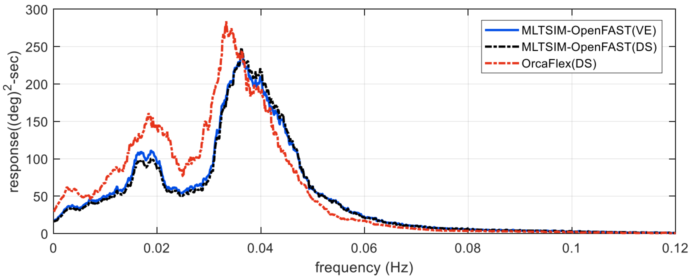


Fig. 27 Line #1 Mooring Tension PSD in Extreme Condition

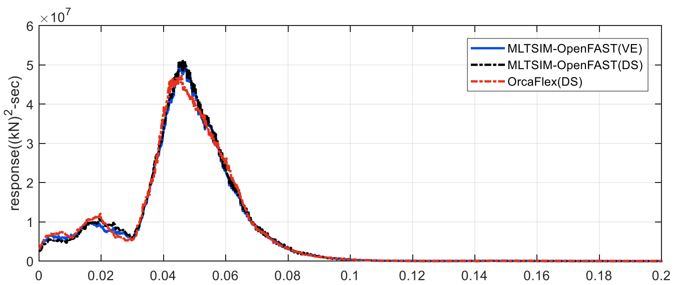


Fig. 28 Wave Elevation PSD in Extreme Condition

Table 8 Statistics of Motions, Mooring Tension, and Internal Loading on Tower Base in the Extreme Condition

| Title | | Unit | Mean | Max | STD |
|---|---|---|---|---|---|
| Wave | MLTSIM-OpenFAST | (m) | 0.00 | 12.61 | 3.12 |
| | OrcaFlex (DS) | (m) | 0.00 | 12.00 | 3.15 |
| Surge | MLTSIM-OpenFAST (VE) | (m) | 8.72 | 30.26 | 3.60 |
| | MLTSIM-OpenFAST (DS) | (m) | 6.02 | 25.05 | 3.59 |
| | OrcaFlex (DS) | (m) | 6.71 | 21.18 | 3.55 |
| Heave | MLTSIM-OpenFAST (VE) | (m) | 0.00 | -10.03 | 2.37 |
| | MLTSIM-OpenFAST (DS) | (m) | -0.25 | -9.40 | 2.36 |
| | OrcaFlex (DS) | (m) | -0.33 | -9.19 | 2.42 |
| Pitch | MLTSIM-OpenFAST (VE) | (deg) | -1.12 | -15.65 | 2.40 |
| | MLTSIM-OpenFAST (DS) | (deg) | -1.07 | -13.89 | 2.37 |
| | OrcaFlex (DS) | (deg) | -2.31 | -17.02 | 2.57 |
| Line1 Tension | MLTSIM-OpenFAST (VE) | (kN) | 3.28E+03 | 9.97E+03 | 1.19E+03 |
| | MLTSIM-OpenFAST (DS) | (kN) | 4.04E+03 | 9.98E+03 | 1.19E+03 |
| | OrcaFlex (DS) | (kN) | 4.05E+03 | 9.45E+03 | 1.19E+03 |
| FA Shear Force | MLTSIM-OpenFAST (VE) | (kN) | 6.97E+02 | 6.84E+03 | 1.43E+03 |
| | OrcaFlex | (kN) | 1.40E+03 | 8.75E+03 | 1.52E+03 |
| Axial Shear Force | MLTSIM-OpenFAST (VE) | (kN) | -1.72E+04 | -1.36E+04 | 9.36E+02 |
| | OrcaFlex | (kN) | -1.80E+04 | -1.36E+04 | 9.84E+02 |
| FA Bending Moment | MLTSIM-OpenFAST (VE) | (kN-m) | 4.11E+04 | 6.32E+05 | 1.36E+05 |
| | OrcaFlex | (kN-m) | 5.78E+04 | 7.61E+05 | 1.47E+05 |

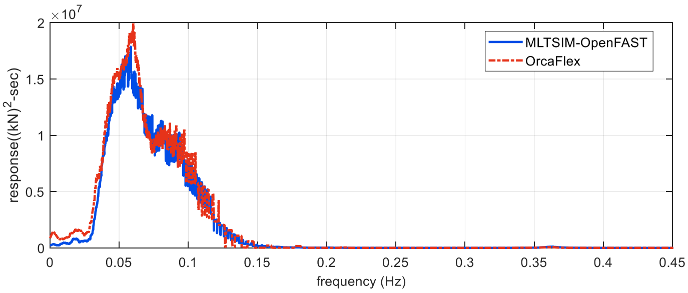


Fig. 29 Axial Force PSD on Tower Base in Extreme Condition

## 7. Conclusions

Precise and reliable numerical modeling of Floating Offshore Wind Turbines (FOWTs) has become critical as their deployment is expected to increase significantly beyond the continental shelves in the USA and globally. Accurate modeling of environmental loadings and the resulting

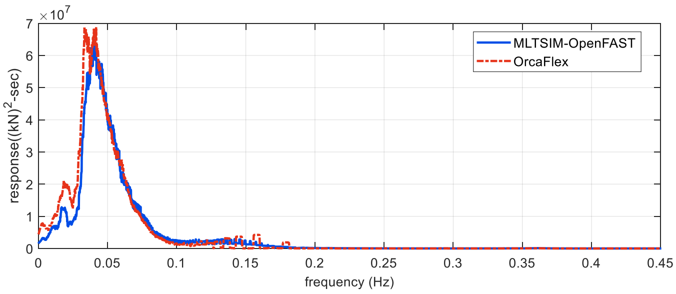


Fig. 30 Fore-Aft Bending Moment PSD on Tower Base in Extreme Condition

dynamic responses are essential for the structural design, operation, and safety of FOWTs. To meet this need, a collaborative project was undertaken involving Texas A&M University, Technip Energies, and the American Bureau of Shipping, with support from the Ocean Energy Safety Institute. The project aimed to develop DT models that could enhance the design and safety of FOWTs by integrating high-fidelity CFD models with mid-fidelity potential-flow models.

The paper presented the development and validation of two mid-fidelity DT models: OrcaFlex and MLTSIM-OpenFAST, specifically for a 15MW semi-submersible wind turbine model for 1000m water depth in Northern California. These models simulate the dynamic interactions between the wind turbine and its platform with a mooring system. The validation process involved several system identification tests and simulations of the FOWT under operational and extreme conditions. The results demonstrated that both mid-fidelity DT models developed could effectively capture the dynamic responses of FOWTs, with the simulations verified through static offset and free decay tests, as well as white-noise and irregular wave simulations. Overall, the results show strong agreement between MLTSIM-OpenFAST and OrcaFlex simulations. Thus, this paper presented an accurate representation of the non-linear dynamics inherent in FOWTs through mid-fidelity potential-flow models.

Future work will be undertaken to extend the capabilities of these models to consider the effects of submarine earthquakes and tsunami waves, expanding the design loading cases of current design guidelines. This study represents a significant advancement in the field of offshore wind energy development, providing a robust framework for the design and maintenance of FOWTs in increasingly challenging environments.

## Acknowledgments

The authors extend their gratitude to the Ocean Energy Safety Institute (OESI) at Texas A&M University (TAMU) sponsored by US Department of Energy (DOE) and Department of the Interior (DOI) for their support of the present study. They also would like to thank Technip Energies (T.EN) and Ekwil for granting permission to publish this paper. Additionally, the authors appreciate Dr. Xiaohong Chen of American Bureau of Shipping (ABS) for her thorough review and recommendation on the present study.

## References

ABS. (2024), "ABS Guide for Building and Classing Floating Offshore Wind Turbines", January 2024.

ABS. (2023), "ABS Guidance Notes on Global Performance and Integrated Load Analysis for Offshore Wind Turbines", August 2023.

ABS. (2012), "ABS Technical Report - Floating Wind Turbines", BSEE TA&R669, Houston (TX), USA

Branlard, E., Jonkman, J., Brown, C. and Zhang, J. (2024), "A digital twin solution for floating offshore wind turbines validated using a full-scale prototype", *Wind Energ. Sci*., **9**(1), 1-24.

Goupee, A., Koo, B., Lambrakos, K., Kimbell, R. and Dagher, H. (2012), "Experimental comparison of three floating wind turbine concepts", *Proceedings of the ASME 31st International Conference on Ocean, Offshore and Arctic Engineering*, Rio de Janeiro, Brazil, 1-6 July, OMAE2012-83645.

Jonkman, J.M. and Matha, D. (2011), "Dynamics of offshore floating wind turbines—analysis of three concepts", *Wind Energy*, **14**(4), 557-569.

Kim, H.C., Kim, K.H., Kim, M.H. and Hong, K. (2017), "Global performance of a KRISO semisubmersible multiunit floating offshore wind turbine: Numerical simulation vs. model test", *Int. J. Offshore Polar Eng*., **27**(1), 70-81.

Kim, H.C. and Kim, M.H. (2016), "Comparison of simulated platform dynamics in steady/dynamic winds and irregular waves for OC4 semi-submersible 5 MW wind-turbine against DeepCwind model-test results", *Ocean Syst. Eng*., **6**(1), 1-21.

Koo, B., Goupee, A., Lambrakos, K. and Kimbell, R. (2012), "Model tests for a floating wind turbine on three different floaters", *Proceedings of the ASME 31st International Conference on Ocean, Offshore and Arctic Engineering*, Rio de Janeiro, Brazil, OMAE2012-83642.

Koo, B., Goupee, A., Lambrakos, K. and Lim, H.J. (2013), "Model test correlation study for a floating wind turbine on a tension leg platform", *Proceedings of the ASME 32nd International Conference on Ocean, Offshore and Arctic Engineering*, Nantes, France, 9-15 June, OMAE2013-1590.

Koo, B., Goupee, A., Lambrakos, K. and Lim, H.J. (2014), "Model test data correlations with fully coupled hull/mooring analysis for a floating wind turbine on a semi-submersible platform", *Proceedings of the ASME 33rd International Conference on Ocean, Offshore and Arctic Engineering*, San Francisco, 8-13 June, OMAE2014-24254.

Koo, B., Jeong, C., Kim, H.C., Lim, H.J., Lai, L. and Jang, H.C. (2022), "Life cycle response analysis of a floating offshore wind turbine", *Proceedings of the ASME 41st International Conference on Ocean, Offshore and Arctic Engineering*, Hamburg, Germany, 5-11 June, OMAE2022-80112.

Lee, I., Kim, M. and Jin, C. (2025), "Impact of hull flexibility on the global performance of a 15 MW concrete-spar floating offshore wind turbine", *Mar. Struct*., **100**, 103724.

Liu, Y., Zhang, J.M., Min, Y.T., Yu, Y., Lin, C. and Hu, Z.Z. (2023), "A digital twin-based framework for simulation and monitoring analysis of floating wind turbine structures", *Ocean Eng*., **283**, 115009.

Orcina, L. (2018), OrcaFlex user manual: OrcaFlex version 10.2 c. Daltongate Ulverston Cumbria, UK.

Pell, J. (2023), "Orcina Project 1512: Comparison of loads from OrcaFlex and OpenFAST for the IEA 15 MW RWT", Orcina, Ltd.

Robertson, A. and Bergua, R. (2023), OC6 Project Phase IV: Validation of Numerical Models for Novel Floating Offshore Wind Support Structures. Pacific Northwest National Laboratory (PNNL), Richland, WA (United States). Atmosphere to Electrons (A2e) Data Archive and Portal.

Webster, W.C., Lambrakos, K., Kim, J.W. and Jing, X. (2012), "Rod dynamics with large stretch", *Proceedings of the International Conference on Offshore Mechanics and Arctic Engineering 2012 Jul 1* **44922**, 345-354. American Society of Mechanical Engineers.

*PS*